Dependence of Sea Ice Yield-Curve Shape on Ice Thickness

ALEXANDER V. WILCHINSKY* AND DANIEL L. FELTHAM

Centre for Polar Observation and Modelling, Department of Space and Climate Physics, University College London, London, United Kingdom

31 October 2003 and 28 June 2004

ABSTRACT

In this note, the authors discuss the contribution that frictional sliding of ice floes (or floe aggregates) past each other and pressure ridging make to the plastic yield curve of sea ice. Using results from a previous study that explicitly modeled the amount of sliding and ridging that occurs for a given global strain rate, it is noted that the relative contribution of sliding and ridging to ice stress depends upon ice thickness. The implication is that the shape and size of the plastic yield curve is dependent upon ice thickness. The yield-curve shape dependence is in addition to plastic hardening/weakening that relates the size of the yield curve to ice thickness. In most sea ice dynamics models the yield-curve shape is taken to be independent of ice thickness. The authors show that the change of the yield curve due to a change in the ice thickness can be taken into account by a weighted sum of two thickness-independent rheologies describing ridging and sliding effects separately. It would be straightforward to implement the thickness-dependent yield-curve shape described here into sea ice models used for global or regional ice prediction.

1. Introduction

Since the pioneering work of Coon et al. (1974) and Hibler (1979), sea ice has been modeled as a plastic material on the large scale (e.g., 100 km) with either elastic or viscous subyield behavior. The hypothesis of plasticity was partly motivated by observations of the discontinuous deformation (failure) of the sea ice cover despite reasonably continuous air and ocean drag forces, pressure-ridging calculations that demonstrated energy required for deformation to be independent of strain rate magnitude (Rothrock 1975), and visual similarities of the sea ice cover to soil, which has been successfully modeled as a granular plastic. Rothrock (1975) related the yield-curve shape to ice thickness redistribution during pressure ridging.

The dependence of ice stress on ice thickness depends upon the mode of failure. During pressure ridging, the ice cover first breaks in flexure into blocks and the ice stress is determined by the work required to move the ice blocks against ridging friction and gravity forces to form a pressure ridge. The ridging stress may be calculated using a model of the redistribution of ice of various thicknesses (e.g., Hibler 1985). In a two-level sea ice dynamics model, however, with two constituents, thin ice/open water and thick ice described by its mean thickness, ridging redistributes thin ice into thick ice. Assuming that the thickness of the lead ice being ridged is proportional to the mean ice thickness h as $h_l = \xi h (\xi < 1)$, and the lead ice redistributes into the ice of mean thickness, the ridging stress is proportional to h^2, as found by Rothrock (1975). This has led some researchers to let the plastic yield curve of sea ice have a quadratic dependence on mean ice thickness (e.g., Overland and Pease 1988; Holland 2001). Because of the random orientation of floe edges, ridging also occurs in shear with the ice-area loss balanced by open-water formation. In the absence of pressure ridging, however, with sliding of floes past each other, the ice stress is determined by the sliding friction between adjacent floe edges (e.g., Tremblay and Mysak 1997) and is proportional to mean ice thickness. A linear dependence of ice stress on mean ice thickness also follows if one assumes that sea ice stress is related to the fracture stress of sea ice as measured in laboratory experiments (Schulson and Nickolayev 1995; Hibler and Schulson 1997, 2000), although scale effects will be important (Dempsey 2000), and in laboratory experiments the aspect ratio of ice samples is much greater than the aspect ratio of a floe (about 1 m/1 km = 10^{-3}). Despite the different dependence of ice stress on mean ice thickness for different failure mechanisms, in two-level sea ice dynamics models the ice stress (plastic yield-curve size) is typically taken to be proportional to mean ice thickness with the coeffi-

* Permanent affiliation: Institute of Mathematics and Mechanics, Kazan State University, Kazan, Republic of Tatarstan, Russia.

Corresponding author address: D. L. Feltham, CPOM, Department of Space and Climate Physics, UCL, Gower Street, London WC1E 6BT, United Kingdom.
E-mail: daniel.feltham@cpom.ucl.ac.uk

cient dependent on the areal fraction of ocean covered in sea ice, A.

2. Yield-curve shape and size dependence

The sea ice cover deforms through simultaneous ridging and sliding of floes past each other, and Pritchard (1981) found stress from sliding friction to be significant. The energy dissipation due to sliding friction was parameterized as a constant fraction of the ridging energy dissipation by Flato and Hibler (1995). Ukita and Moritz (1995, 2000) and Moritz and Ukita (2000) generalized the approach of Rothrock (1975) by relating the energy of deformation to the amount of ridging and sliding that occurs in an idealized ice cover for a given global strain rate. In their work, the ratio between the energy dissipation in ridging and sliding is not constant but depends on the deformation type. They relate the work done by internal sea ice forces to the ridging function $\alpha_r(\theta)$ describing how much of the full strain rate goes into ridging (as in Rothrock 1975) and a sliding function $\alpha_s(\theta)$ describing how much of the full strain rate goes into sliding. The angle $\theta = \arctan(\dot{\epsilon}_{II}/\dot{\epsilon}_I)$ is the ratio of the second and first strain rate invariants (maximum shear rate and divergence, respectively) and determines the relative amount of shear to divergence. Note that $\theta = 0$ in pure divergence, $\theta = \pi/4$ in uniaxial extension, $\theta = \pi/2$ in pure shear, $\theta = 3\pi/4$ in uniaxial contraction, and $\theta = \pi$ for pure convergence. The rate of work done by ice stresses in deformation of the ice cover per unit time can be written as

$$\overline{\sigma}_I\dot{\epsilon}_I + \overline{\sigma}_{II}\dot{\epsilon}_{II} = |\dot{\epsilon}|[P_r\alpha_r(\theta) + P_s\alpha_s(\theta)], \qquad (1)$$

where $|\dot{\epsilon}| = (\dot{\epsilon}_I^2 + \dot{\epsilon}_{II}^2)^{1/2}$ and bars show dimensional stress. In this equation, P_r and P_s are the ridging and sliding strengths, respectively. Generally, there is sliding of floes past each other, even in pure convergence. This is because, as the ice floe centers approach each other, there is a nonzero component of this motion along the floe boundary (i.e., sliding). This is not the case, however, if the floe boundary is perpendicular to the vector joining the floe centers, as in the case of a regular tiling of the ocean with square ice floes (Moritz and Ukita 2000), in which case $\dot{\epsilon}_{II} = \alpha_s = 0$, $|\dot{\epsilon}| = |\dot{\epsilon}_I|$, and $\alpha_r(\theta) = 1$, so that $\overline{\sigma}_I = P_r$. We take the ridging strength to depend quadratically on ice thickness in common with Overland and Pease (1988) and represent it as $P_r = H^2 f_r(A)P_r^*$, where $H = h/1$ m and P_r^* is the maximum ridging strength, being the pressure necessary to form pressure ridges from ice of 1-m thickness under pure convergence without interfloe sliding (tiling of regular sea ice floes). The function $f_r(A)$, where $f_r(0) = 0$ and $f_r(1) = 1$, describes the influence of the sea ice concentration on the ridging strength. Because of the linear dependence of the sliding friction on mean ice thickness, we write the sliding strength as $P_s = Hf_s(A)P_s^*$, where P_s^* is the maximum sliding strength, being the sliding stress for 1-m-thick ice, where the floe–floe boundary of a square tiling is at angle $\pi/4$ to the principal strain-rate axes. In this case, the deformation occurs because of sliding only (Moritz and Ukita 2000) so that $\dot{\epsilon}_I = \alpha_r = 0$, $|\dot{\epsilon}| = |\dot{\epsilon}_{II}|$, and $\alpha_s(\theta) = 1$, and thus $\overline{\sigma}_{II} = P_s = P_s^*$. The function f_s describes the influence of sea ice area concentration on sliding stress [$f_s(0) = 0$, $f_s(1) = 1$]. The sliding friction depends on the applied normal stress through the friction proportionality coefficient k so that, if there is no ridging, frictional sliding of floes past each other can occur for any shear strength lying between zero, when no pressure is applied, up to kP_r^*, when ridging starts to occur. Therefore an evaluation of the sliding contribution to the work done by sea ice deformation is possible only if it is assumed that all sliding surfaces are under ridging pressure, in which case $P_s^* = kP_r^*$. We set $f_r = f_s \equiv f$ so that for unit ice thickness k is the ratio of energy transformed in frictional sliding of floes past each other to pressure ridge formation and, therefore, has the same physical significance as the k that appears in Ukita and Moritz's plastic work equation (Ukita and Moritz 1995, 2000). Note that as the ridging stress acting on 1 m of the whole ice thickness is equal to fP_r^*H, the assumption that P_s^* is constant means that the sliding strength only weakly depends on the applied ridging stress for a given ice thickness range.

After nondimensionalizing the stresses by fP_r^*, we can write the rate of work done by ice stresses per unit strain rate as

$$\sigma_I\cos\theta + \sigma_{II}\sin\theta = H^2\left(\alpha_r + \frac{k}{H}\alpha_s\right). \qquad (2)$$

This equation modifies the expression used by Ukita and Moritz (1995, 2000) through inclusion of the dependence of ridging and sliding contributions on the normalized ice thickness H.

The ridging and sliding functions, α_r and α_s, are found from purely kinematic considerations (Ukita and Moritz 2000; Moritz and Ukita 2000). They assumed the ice cover to consist of a tiling of either regular polygons or a random distribution of irregular polygons (generated using the Poisson process). From an imposed global strain rate, they calculated the velocity of each floe and thus determined the opening/closing and sliding rates between adjacent floes. For a random, Poisson distribution of cracks between the floes, Ukita and Moritz (2000) calculated the ridging and sliding functions presented here in Fig. 1. Note that for pure shear $\alpha_r(\pi/2) \neq 0$; therefore for a general floe configuration both sliding and ridging occur in pure shear.

Ukita and Moritz [2000, their (8)] minimized the maximum shear stress σ_{II} [given by simple rearrangement of (2)] for a particular σ_I with respect to θ to determine the yield curve

$$\left\{\sigma_I, \min_\theta \sigma_{II}(\sigma_I, \theta)\right\}. \qquad (3)$$

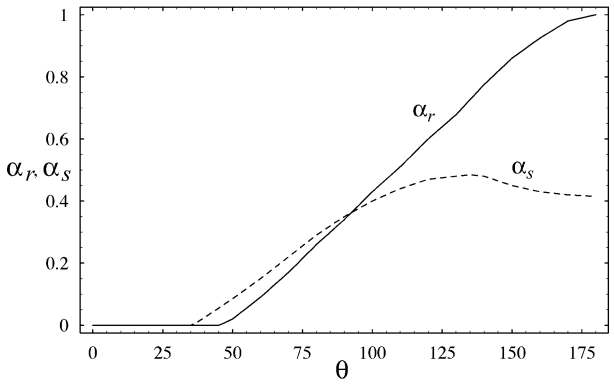

FIG. 1. Ridging function $\alpha_r(\theta)$ (solid line) and sliding function $\alpha_s(\theta)$ (dashed line) as found by Ukita and Moritz (2000) for Poisson distribution of cracks.

Here, we repeat this process to determine a set of yield curves for the set of ice thicknesses $H = \{0.3, 0.6, 1, 2.5, 5\}$ and $k = 1$ presented in Fig. 2 in normalized form [$\sigma_{I\max} = \max_\theta|\sigma_I| = |\sigma_I(\theta = \pi)|$, $\sigma_{II\max} = \max_\theta|\sigma_{II}|$]. We can see that the yield-curve shape clearly depends upon ice thickness, as expected from (2): An increase of ice thickness leads to a decrease in the relative importance of the sliding stress contribution to that of ridging and vice versa. The yield-curve shape is most sensitive to variation in ice thickness at about $\sigma_I/\sigma_{II\max} \approx -0.8$ with the normalized shear stress here varying by up to 20% for the thickness range considered.

The change of the size of the yield curve, expressed through the value of $\sigma_{I\max}$, as H is varied is shown in Fig. 3. For comparison we also show how the yield-curve size would change if the yield-curve shape did not change. For this purpose we consider the stress

$$\boldsymbol{\sigma}^* = H^\gamma \boldsymbol{\sigma}(H = 1), \tag{4}$$

where $\boldsymbol{\sigma}$ is our solution given by (2) and (3), and plot $\sigma^*_{I\max}$ for $\gamma = 2$ (quadratic dependence, dashed curve) and $\gamma = 1$ (linear dependence, dotted–dashed curve).

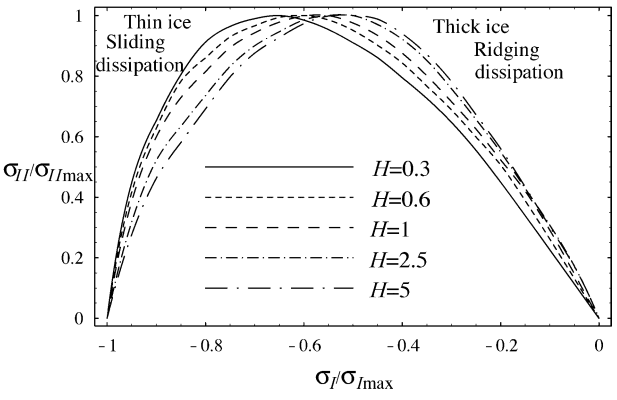

FIG. 2. Normalized yield curves for $H = 0.3$ (solid line), $H = 0.6$ (short dashed), $H = 1$ (long dashed), $H = 2.5$ (dot–short dashed), and $H = 5$ (dot–long dashed).

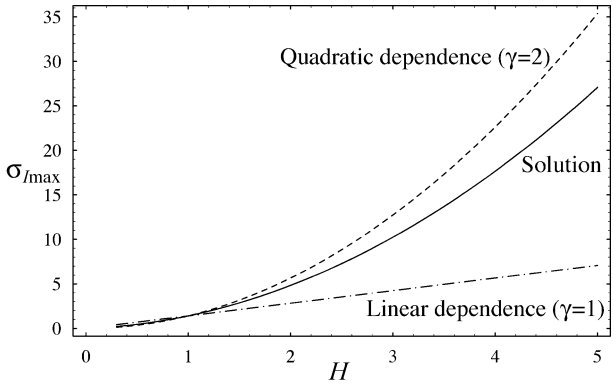

FIG. 3. Size of the yield curve expressed through the magnitude of the normal stress in convergence, $\sigma_{I\max} = |\sigma_I(\theta = \pi)|$ for solution (7) with $k = 1$ (solid line), and the cases of constant yield-curve shape with quadratic dependence on the ice thickness ($\gamma = 2$) in (4) (dashed line) and linear dependence ($\gamma = 1$) (dotted–dashed line). The yield curves coincide at $H = 1$.

It can be seen that the difference between the dependence of ridging and sliding energy dissipation on the mean ice thickness affects not only the shape of the yield curve, but also its size. The normalized difference between the constant-shape yield curves given by $\boldsymbol{\sigma}^*$ and the yield curve given by $\boldsymbol{\sigma}$ is illustrated in Fig. 4, where $\sigma^*_{I\max}/\sigma_{I\max}$ is plotted. The deviation of the constant-shape yield-curve size from our proposed yield curve is about 20%–30% for the quadratic dependence ($\gamma = 2$) and can exceed 50% for the linear dependence ($\gamma = 1$) for the range of thicknesses considered.

3. Decomposition of yield stress into ridging and frictional sliding contributions

In order to avoid complete recalculation of the yield curve every time the ice thickness changes, we consider the two yield curves obtained by respective neglect of

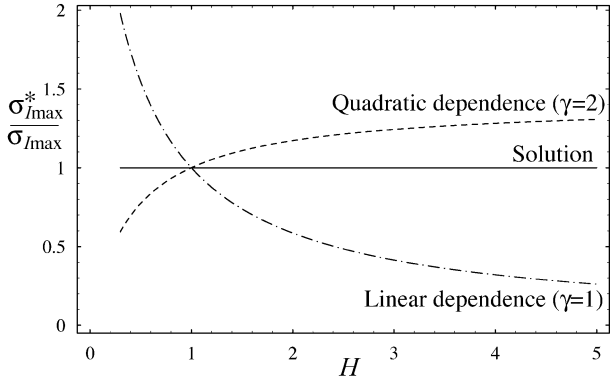

FIG. 4. Relative deviation of the constant yield-curve size from that given by the solution (7), $\sigma^*_{I\max}/\sigma_{I\max} = |\sigma^*_I(\theta = \pi)|/|\sigma_I(\theta = \pi)|$, for the quadratic dependence on the ice thickness ($\gamma = 2$) given by the dashed line, and linear ($\gamma = 1$) given by the dotted–dashed line. The solution (7) is normalized to unity.

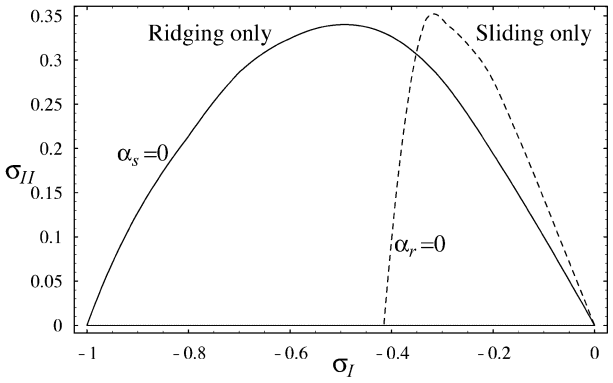

FIG. 5. Yield curves for ridging only (solid line) and sliding only (dashed line).

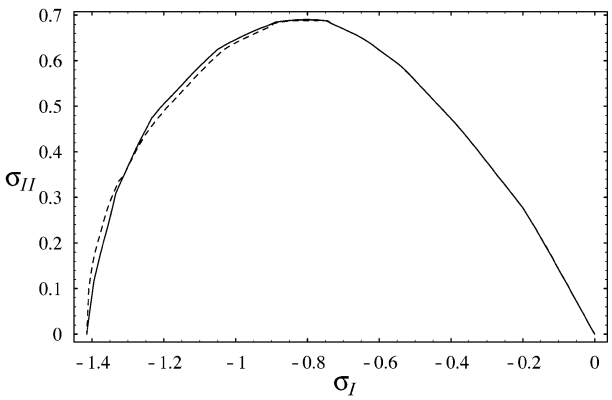

FIG. 6. Comparison of yield curve obtained solving the full system, (2) (solid line), and that obtained by adding the separate ridging and sliding yield-curve contributions (dashed line) with $H = k = 1$.

either sliding function (and setting $kH = 1$) or ridging function (and setting $H = 1$), respectively:

$$\sigma_I^r \cos\theta + \sigma_{II}^r \sin\theta = \alpha_r(\theta) \quad \text{and} \tag{5}$$

$$\sigma_I^s \cos\theta + \sigma_{II}^s \sin\theta = \alpha_s(\theta), \tag{6}$$

where σ_I^r, σ_{II}^r and σ_I^s, σ_{II}^s describe the yield curves presented in Fig. 5 determined from the minimization of $\sigma_{II}^r(\theta, \sigma_I^r)$ and $\sigma_{II}^s(\theta, \sigma_I^s)$ with respect to θ, respectively. The shape of the yield curve for the stress $\boldsymbol{\sigma}^r$ corresponds to that found by Ukita and Moritz (2000, their Fig. 3) for their $k = 0$, while the shape of the yield curve for the stress $\boldsymbol{\sigma}^s$ can be found if their $k \to +\infty$. The sliding yield curve is asymmetric, with the maximum sliding stress closer to the maximum compressive stress than zero compressive stress. This is because the sliding function $\alpha_s(\theta)$ determining the stress does not change significantly as θ increases from $\pi/2$ (pure shear) to π (pure convergence), as an increase of sliding due to convergence of irregularly shaped ice floes is counteracted by its decrease due to smaller shearing deformation. If we assume that the stress tensors can be written as $\boldsymbol{\sigma}^r = \boldsymbol{\sigma}^r(\dot{\boldsymbol{\epsilon}})$ and $\boldsymbol{\sigma}^s = \boldsymbol{\sigma}^s(\dot{\boldsymbol{\epsilon}})$, then we can introduce the stress tensor

$$\boldsymbol{\sigma}^a(\dot{\boldsymbol{\epsilon}}) = H^2\boldsymbol{\sigma}^r(\dot{\boldsymbol{\epsilon}}) + kH\boldsymbol{\sigma}^s(\dot{\boldsymbol{\epsilon}}), \tag{7}$$

which satisfies the normalized equation in (2), because $\boldsymbol{\sigma}^r(\dot{\boldsymbol{\epsilon}})$ and $\boldsymbol{\sigma}^s(\dot{\boldsymbol{\epsilon}})$ have the same principal axes, $\sigma_I^a = H^2\sigma_I^r + kH\sigma_I^s$ and $\sigma_{II}^a = H^2\sigma_{II}^r + kH\sigma_{II}^s$. Moreover, because $\sigma_I^a(\theta)$ is a monotone function, for a particular value $\sigma_I \geq \sigma_I^a(\pi)$ we can find θ_0 such that $\sigma_I = \sigma_I^a(\theta_0)$. In this case we can rewrite the yield curve (3) as

$$\left\{\sigma_I^a(\theta_0), \min_\theta \langle H^2\sigma_{II}^r[\theta, \sigma_I^r(\theta_0)] + kH\sigma_{II}^s[\theta, \sigma_I^s(\theta_0)]\rangle\right\}. \tag{8}$$

Because both $\sigma_{II}^r[\theta, \sigma_I^r(\theta_0)]$ and $\sigma_{II}^s[\theta, \sigma_I^s(\theta_0)]$ are minimized by $\theta = \theta_0$, the yield curve for the full solution, (3), is determined as

$$\left\{\sigma_I^a, \min_\theta \sigma_{II}^a(\sigma_I^a, \theta)\right\}. \tag{9}$$

Since both $\boldsymbol{\sigma}$ and $\boldsymbol{\sigma}^a$ satisfy the same energy balance (2) and the principle of shear stress minimization (3), it follows that $\boldsymbol{\sigma} = \boldsymbol{\sigma}^a$. Numerical calculations, presented in Fig. 6, show that the yield curve derived by solving the full system (2) and that obtained by combining the ridging and sliding yield curves are the same within numerical accuracy. This has been done by minimization of σ_{II}^r and σ_{II}^s with regard to θ for fixed σ_I^r and σ_I^s, respectively. This detemines four functions $\sigma_{II}^r(\theta)$, $\sigma_{II}^s(\theta)$, $\sigma_I^r(\theta)$, and $\sigma_I^s(\theta)$. The yield curve is then obtained by plotting $\{[H^2\sigma_{II}^r(\theta) + kH\sigma_{II}^s(\theta)], [H^2\sigma_I^r(\theta) + kH\sigma_I^s(\theta)]\}$ as θ is varied from 0 to π.

4. Summary

We have shown that, because the energy transformation associated with ridging and sliding depends on the mean ice thickness in different ways, the yield-curve shape changes with ice thickness. The yield-curve size typically deviates by more than 20% from those given by the constant yield-shape curves with either linear or quadratic size dependence on ice thickness. A straightforward way to calculate the shape-dependent yield curve is by summation of the separate contributions of ridging and sliding, weighted by the thickness-dependent coefficients H^2 and kH. The approach we have presented here can be extended to a multiple-thickness distribution theory.

Acknowledgments. This work is funded by NERC UK.

REFERENCES

Coon, M. D., G. A. Maykut, R. S. Pritchard, D. A. Rothrock, and A. S. Thorndike, 1974: Modeling the pack sea ice as an elastic-plastic material. *AIDJEX Bull.,* **24,** 1–105.

Dempsey, J. P., 2000: Research trends in ice mechanics. *Int. J. Solids Structures,* **37,** 131–153.

Flato, G. M., and W. D. Hibler III, 1995: Ridging and strength in modelling the thickness distribution of Arctic sea ice. *J. Geophys. Res.,* **100,** 18 611–18 626.

Hibler, W. D., III, 1979: A dynamic thermodynamic sea ice model. *J. Phys. Oceanogr.,* **9,** 815–846.

——, 1985: Numerical modeling of sea ice dynamics and ice thickness characteristics. CRREL Rep. 5, 51 pp.

——, and E. M Schulson, 1997: On modelling sea ice fracture and flow in numerical investigation of climate. *Ann. Glaciol.,* **25,** 26–32.

——, and ——, 2000: Anisotropic failure and flow of flawed sea ice. *J. Geophys. Res.,* **105,** 17 105–17 120.

Holland, D. M., 2001: An impact of subgrid-scale ice–ocean dynamics on sea-ice cover. *J. Climate,* **14,** 1585–1601.

Moritz, R. E., and J. Ukita, 2000: Geometry and the deformation of pack ice: I. A simple kinematic model. *Ann. Glaciol.,* **31,** 313–322.

Overland, J. E., and C. H. Pease, 1988: Modeling ice dynamics of coastal seas. *J. Geophys. Res.,* **93,** 15 619–15 637.

Pritchard, R. S., 1981: Mechanical behaviour of pack ice. *Mechanics of Structured Media: Proceedings of the International Symposium on the Mechanical Behavior of Structured Media,* Part A, A. P. S. Selvadurai, Ed., Elsevier, 49–61.

Rothrock, D. A., 1975: The energetics of the plastic deformation of pack ice by ridging. *J. Geophys. Res.,* **80,** 4514–4519.

Schulson, E. M., and O. Y. Nickolayev, 1995: Failure of columnar saline ice under biaxial compression: Failure envelopes and the brittle-to-ductile transition. *J. Geophys. Res.,* **100,** 22 383–22 400.

Tremblay, L. B., and L. A. Mysak, 1997: Modelling sea ice as a granular material, including the dilatancy effect. *J. Phys. Oceanogr.,* **27,** 2342–2360.

Ukita, J., and R. E. Moritz, 1995: Yield curves and flow rules of pack ice. *J. Geophys. Res.,* **100,** 4545–4557.

——, and ——, 2000: Geometry and the deformation of pack ice. II. Simulation with a random isotropic model and implementation in sea-ice rheology. *Ann. Glaciol.,* **31,** 323–326.